RESEARCH ARTICLE

Molecular Characterization of HLA-B27 in Anterior Uveitis: Integrated Serological and Genetic Analysis Reveals Elevated Antigen Levels and Variants Concentrated in Exons 2 and 3

Shinta Stri Ayuda Nur Setyaningsih[1,2], Arief Akhdestira Mustaram[2,3], Angga Fajriansyah[2,3], Patriotika Muslima[2,3], Elfa Ali Idrus[2,3], Muhammad Hamzah Syaifullah Azmi[1], Elsa Gustianty[2,3], Ernawati Arifin Giri-Rachman[1], Marselina Irasonia Tan[1,*]

[1]School of Life Sciences and Technology, Institut Teknologi Bandung, Jl. Ganesa 10, Lebak Siliwangi, Coblong, Bandung 40135, Indonesia
[2]National Eye Center, Cicendo National Eye Hospital, Jl. Cicendo 4, Babakan Ciamis, Sumur Bandung, Bandung 40117, Indonesia
[3]Department of Ophthalmology, Faculty of Medicine, Padjadjaran University, Jl. Cicendo 4, Babakan Ciamis, Sumur Bandung, Bandung 40117, Indonesia

*Corresponding author. Email: marsel@itb.ac.id

Received date: May 27, 2026; Revised date: Jun 26, 2026; Accepted date: Jun 29, 2026

Abstract

BACKGROUND: Anterior uveitis is the most common form of intraocular inflammation and an important cause of visual morbidity worldwide. Human leukocyte antigen B27 (HLA-B27) is a well-established immunogenetic risk factor; however, its molecular diversity remains insufficiently characterized in Indonesian populations. This study was conducted to characterize HLA-B27 at both the serological and genetic levels by quantifying serum antigen levels and identifying sequence variations in the *HLA-B27* gene associated with anterior uveitis in Indonesian patients.

METHODS: Thirteen anterior uveitis patients who were clinically evaluated through the Standardization of Uveitis Nomenclature (SUN) criteria were involved in this study. Blood sample was collected from subjects, and serum HLA-B27 concentrations were measured by enzyme-linked immunosorbent assay (ELISA). Genomic DNA was analyzed using combined Sanger and Oxford Nanopore sequencing. Variant calling and annotation were performed using a custom bioinformatics pipeline.

RESULTS: Serum HLA-B27 antigen levels were significantly higher in anterior uveitis patients than in healthy reference controls. Sequence analysis identified 43 patient-exclusive variants after exclusion of shared polymorphic changes, from which 13 recurrent or potentially functionally relevant variants were prioritized for downstream analysis. These variants were predominantly distributed within exons 2 and 3 and comprised single-nucleotide substitutions, coding-region insertion–deletion events, and one promoter-region insertion. Several coding variants resulted in amino acid substitutions, while adjacent compensatory indel pairs were also identified among exon 2 frameshift-associated variants.

CONCLUSION: Anterior uveitis is associated with both elevated circulating HLA-B27 antigen levels and sequence variation within functionally important regions of the *HLA-B27* gene, particularly exons 2 and 3. The identified missense substitutions, coding-region indels, and promoter insertion suggest potential effects on peptide binding, molecular stability, immune interaction, intracellular protein handling, or transcriptional regulation.

KEYWORDS: anterior uveitis, HLA-B27, genomic variants, peptide-binding groove, protein misfolding

Indones Biomed J. 2026; 18(3): 299-311

Introduction

Uveitis comprises a heterogeneous group of intraocular inflammatory disorders that threaten vision and remain a major cause of ocular morbidity worldwide.(1) Based on anatomical classification, uveitis is divided into anterior, intermediate, posterior, and panuveitis, with anterior uveitis representing the most common form.(2) Globally, the incidence of uveitis ranges from approximately 50 to over 200 cases per 100,000 person-years, underscoring its relevance as a public health concern.(3)

The burden is particularly evident in developing regions, including Southeast Asia, where hospital-based studies in Indonesia report anterior uveitis as one of the most frequently encountered forms of intraocular inflammation in tertiary eye care settings. (4) Similar patterns are observed in other countries, including China and India, where prevalence in referral centers is disproportionately high relative to population-based estimates due to referral bias, delayed diagnosis, and a higher burden of immune-mediated disease.(5,6) Uveitis also accounts for approximately 25–35% of visual impairment cases in developing countries, depending on access to care and underlying etiologies.(7,8) Importantly, uveitis predominantly affects individuals aged 20–50 years, thereby contributing substantially to socioeconomic burden. (9)

Etiologically, uveitis may arise from infectious or non-infectious causes, the latter often involving immune-mediated and autoimmune processes.(10) Non-infectious anterior uveitis is frequently associated with systemic inflammatory diseases such as ankylosing spondylitis, Behçet's disease, and Vogt–Koyanagi–Harada disease, reflecting systemic immune dysregulation. Clinically, anterior uveitis can lead to complications such as posterior synechiae, band keratopathy, cataract, and elevated intraocular pressure resulting in secondary glaucoma.(11-14) These manifestations underscore the importance of understanding the underlying biological mechanisms of ocular inflammation. Among genetic factors, the association between anterior uveitis and human leukocyte antigen B27 (HLA-B27) is one of the most consistent findings in ocular immunology.(15)

At the molecular level, HLA-B27 is a polymorphic class I major histocompatibility complex (MHC) molecule that presents antigenic peptides to class of differentiation (CD)8^+ T cells.(16) The gene comprises seven exons, with exons 2 and 3 encoding the α1 and α2 domains that form the peptide-binding groove and determine antigen specificity. (17) Polymorphisms within these regions may alter peptide binding, affect protein folding stability, and modulate immune responses. These variations have been proposed to contribute to disease pathogenesis through mechanisms such as aberrant antigen presentation, protein misfolding, and induction of endoplasmic reticulum stress.(16,17)

Consistent with these mechanisms, HLA-B27–associated anterior uveitis is typically acute, recurrent, and often unilateral, occurring either independently or alongside systemic spondyloarthropathies. However, despite this well-established association, the molecular diversity of HLA-B27, particularly at the sequence level, remains incompletely characterized across populations.(18) This gap is especially relevant in Southeast Asia, especially Indonesia, where genetic diversity is high but data on *HLA-B27* variation remain limited.(19) Population-specific characterization is therefore essential to better understand disease susceptibility and phenotype caused by anterior uveitis.

Therefore, this study was conducted to provide an integrative molecular characterization of HLA-B27 in Indonesian patients with anterior uveitis. *HLA-B27* sequences were obtained using a combined Sanger and Oxford Nanopore sequencing approach (20,21), enabling high-resolution detection of nucleotide variants and their potential impact on the encoded protein. A custom bioinformatics pipeline was used for variant identification and annotation, while clinical data, including HLA-B27 antigen expression level and inflammatory grading, were incorporated to provide phenotypic context. This study addresses the lack of population-specific molecular data and establishes a preliminary framework linking *HLA-B27* genetic variation with serological features in anterior uveitis, specifically within the Indonesian population.

Methods

This study was designed as a cross-sectional clinical and molecular investigation of patients with anterior uveitis. Subjects recruitment, clinical assessment, and sample collection were conducted at the Outpatient Department of Infection and Immunology, Cicendo National Eye Hospital, Bandung, Indonesia, while molecular analyses, including ELISA analysis of blood serum HLA-B27, DNA extraction, amplification, and sequencing, were carried out at the School of Life Sciences and Technology, Institut Teknologi Bandung, Indonesia.

Pilot Cohort Study and Eligibility Criteria

Subjects eligible in this study were consecutively recruited based on the following criteria: i) a clinical diagnosis or documented history of acute or recurrent anterior uveitis, defined by a minimum interval of three months between episodes; ii) age between 18 and 60 years; and iii) elevated HLA-B27 antigen levels relative to the reference range, as quantified by ELISA. Subjects' enrollment was carried out between January 2023 and April 2025, and written informed consent was obtained from all subjects before sample collection. A total of 15 subjects were enrolled in the study cohort, comprising 13 anterior uveitis patients and 2 healthy reference individuals.

Blood Samples Collection and Processing

Peripheral venous blood (5–10 mL) was collected from each participant under aseptic conditions and divided into tubes for serological and genomic analyses. For serological assessment, blood was collected in tubes without anticoagulant, allowed to clot at room temperature, and centrifuged at 4,000 rpm for 10 min to obtain serum. Serum aliquots were transferred into sterile microcentrifuge tubes and stored at −20°C for HLA-B27 quantification by enzyme-linked immunosorbent assay (ELISA) or at −80°C for long-term storage. For genomic analysis, blood was collected in EDTA-treated tubes and centrifuged at 4,000 rpm for 5 min to isolate the buffy coat fraction. Buffy coat samples were processed immediately or stored at 4°C for short-term preservation prior to genomic DNA extraction. All samples were labeled using study identifiers and handled in accordance with institutional biosafety and ethical guidelines.

HLA-B27 Antigen Quantification

To evaluate whether anterior uveitis was associated with altered circulating HLA-B27 antigen levels and to complement the genetic analyses, serum HLA-B27 concentrations were quantified using a commercially available sandwich ELISA kit (Human HLA-B27 ELISA Kit, Catalog No. E-EL-H0157; Elabscience Biotechnology Inc., Houston, TX, USA) in accordance with the manufacturer's instructions. The reported assay sensitivity was 0.19 ng/mL, with a detection range of 0.31–20 ng/mL. A standard calibration curve was prepared using serial dilutions of the supplied reference standard (0–20 ng/mL). Serum samples were analyzed in duplicate using the pre-coated microplate format provided in the kit. Absorbance was measured at 450 nm using a calibrated microplate reader following completion of the enzymatic reaction. HLA-B27 concentrations were calculated using a four-parameter logistic (4-PL) regression model, and values were adjusted according to the corresponding sample dilution factor when applicable. Samples exceeding the upper detection limit were reanalyzed following appropriate dilution.

Genomic DNA Extraction

Genomic DNA was extracted from the buffy coat fraction of EDTA-anticoagulated peripheral blood using an automated magnetic bead–based extraction system (TANBead® Nucleic Acid Extraction Kit) in accordance with the manufacturer's instructions. Approximately 300 µL of buffy coat was processed using the manufacturer's BLOOD-AUTO extraction program, which performs automated cell lysis, nucleic acid binding, washing, and elution steps. Purified DNA was quantified using a NanoDrop spectrophotometer (Thermo Fisher Scientific, Waltham, MA USA), and DNA purity was assessed based on the A260/A280 ratio, with values of approximately 1.8 considered acceptable. DNA samples with adequate concentration and purity were aliquoted and stored at −20°C until further use for PCR amplification and sequencing.

Amplification of the *HLA-B27* Gene

Targeted amplification of the *HLA-B27* gene was performed using polymerase chain reaction (PCR) to generate amplicons for downstream Sanger and Oxford Nanopore sequencing. Primers were designed based on the *HLA-B27* reference sequence (GenBank accession number X03945.1) (22) using SnapGene software and the PrimerQuest™ Tool (Integrated DNA Technologies, Coralville, IA, USA) to ensure specific amplification and complete coverage of the target locus. Sanger sequencing was performed for a subset of samples during the initial phase of the study, whereas Oxford Nanopore sequencing was subsequently used for the remaining samples because it enabled higher-throughput analysis and characterization of longer DNA fragments. For Sanger sequencing, a primer-walking strategy was employed using six forward sequencing primers distributed across the amplified region to provide sequential coverage. This approach was applied to two study samples and two non-uveitis reference samples. For Oxford Nanopore sequencing, barcoded primer sets were used to generate long amplicons spanning the target region, enabling multiplexed sequencing of the other 11 study samples. Detailed primer sequences and characteristics were provided in Table 1, while the barcode assignments used for Oxford Nanopore sequencing were provided in Table 2. These unique barcode sequences enabled multiplexed sequencing of multiple samples within

Table 1. Primers used in this study.

Primer ID/Name	Sequence (5'→3')	Length (nt)	%GC	Tm (°C)	Function
FWD-Promotor-HLAB27	ACTCCCACGAGTTTCACTTCTTC	23	47.83	60.49	- Universal FWD - Sanger walking - Nanopore
FWD-Exon2-HLAB27	GACTCAGAATCTCCTCAGACG	21	55.00	55.00	Sanger walking
FWD-Exon3-HLAB27	GCTACTACAACCAGAGCGAG	20	55.00	55.00	Sanger walking
FWD-Exon4-HLAB27	CAGAGACTCGAACTTTCCAATG	22	45.45	57.08	Sanger walking
FWD-Exon5-HLAB27	GAGCAGAGATACACATGCCATG	22	50.00	62.80	Sanger walking
FWD-Exon6-HLAB27	GTCCAAGACGAAGGAGGTTC	19	58.00	55.00	Sanger walking
REV-Terminator-HLAB27	GACCCCAAGAATCTCACCTTTTC	23	47.88	59.24	- Universal REV - Nanopore

a single run and facilitated accurate demultiplexing and read assignment during downstream data analysis.

PCR reactions were performed in a final volume of 25 µL containing GoTaq® Green Master Mix (Promega), 0.2–0.4 µM of each primer, and approximately 50–100 ng of DNA template under optimized thermal cycling conditions as summarized in Table 3. PCR products were resolved on 1–1.5% agarose gels and visualized under UV illumination to confirm amplicon size and specificity. Only products showing a single band of the expected size were used for sequencing.

HLA-B27 Gene Sequencing

To obtain high-confidence reference sequences for initial characterization of *HLA-B27* variation, a subset comprising two anterior uveitis subjetcs and two healthy reference individuals was analyzed using Sanger sequencing. Sanger sequencing was performed by a commercial service provider (1st BASE, Selangor, Malaysia). Purified PCR amplicons as shown in Figure 1, encompassing the target *HLA-B27* locus, were selected based on expected product size (2882 bp) and adequate DNA quality and quantity before submission. A primer-walking strategy employing seven forward sequencing primers was used to provide sequential coverage across the *HLA-B27* gene. Purified amplicons and corresponding primers were submitted for capillary electrophoresis sequencing, and raw chromatogram files were returned for downstream analysis.

Table 2. Barcode assignments used for sample multiplexing and demultiplexing during Oxford Nanopore sequencing.

Barcode ID	Sequence (5'→3')
RB01	AAGAAAGTTGTCGGTGTCTTTGTG
RB02	TTGGATTCTTTTCTTGCTGCGTGT
RB03	GCTCTCTCAAGTCCTCCTATTGTG
RB04	GTGATTCTCGTCTTTCTAGTTGTG
RB05	TCCATCCTCTTTTCCTTAGTAGTG
RB06	GTTGTTGTCTTCCTTTGTTTGTGT
RB07	TCGTTGTCTTCCTTTGTTCGTGTG
RB08	TTGGTTCGTTTCCTTGTTTCTGTG
RB09	AGAGTTCTTCCTTGTTTCTTCGTG
RB10	GCTCGTTCCTTGTTTCTTCCTGTG
RB11	TCCATCCCTTGTTTCCTTCCTGTG

To facilitate full-length characterization of the *HLA-B27* amplicon across the remaining study samples in a scalable and multiplexed manner, Oxford Nanopore sequencing was performed on the remaining 11 anterior uveitis patient samples. Unlike Sanger sequencing, which requires multiple primer-walking reactions to cover the entire 2882 bp target region, Nanopore sequencing enables long-read analysis of the complete amplicon in a single sequencing run while supporting simultaneous processing of multiple barcoded samples. PCR amplicons generated using barcoded primer sets were used as input for Oxford Nanopore sequencing, with each barcode uniquely assigned to an individual sample to enable multiplexed analysis. Following amplification, barcoded amplicons were assessed for DNA concentration and integrity before library preparation. Sequencing libraries were prepared using the Rapid Barcoding Kit (SQK-RBK114.24 or SQK-RBK114.96; Oxford Nanopore Technologies, Oxford, UK) according to the manufacturer's instructions. Sequencing was performed in-house at the School of Life Sciences and Technology, Institut Teknologi Bandung, using a MinION or GridION platform equipped with compatible flow cells. Raw electrical signal data were acquired in real time and basecalled using the Oxford Nanopore software pipeline to generate sequence reads for downstream bioinformatic analysis.

Table 3. Optimized PCR thermal cycling conditions.

Reaction	Temperature	Duration	Cycle
Initial Denaturation	95 °C	02:00	1
Denaturation	95 °C	00:30	35
Annealing	60 °C	00:30	35
Extension	72 °C	01:00	35
Final Extension	72 °C	05:00	1
Hold	4 °C	∞	-

Reads Processing and Variant Calling

Raw Sanger sequencing chromatograms generated from forward walking primers were processed using UGENE software v52.1 (UniPro, Novosibirsk, Russia) . Reads were quality-trimmed using an automated threshold of Q40, assembled into contigs with a minimum mapping similarity of 75%, and used to generate per-sample consensus sequences. Chromatograms were subsequently inspected manually to resolve ambiguous base calls and remove residual low-quality regions. Consensus sequences were aligned to the HLA-B27 reference sequence (GenBank accession number X03945.1) (22) using the MAFFT algorithm implemented in AliView (v3.0). Variants relative to the reference sequence were identified using a custom bioinformatics pipeline.

Oxford Nanopore reads were analyzed using a parallel workflow. Long-read data were aligned to the reference sequence using minimap2, and alignment files were processed with samtools. Variant calling was performed using Clair3 with the Oxford Nanopore–optimized ont_guppy5 model, generating pileup and full-alignment variant call format (VCF) outputs that were subsequently merged to obtain final per-sample calls. To reduce sequencing noise, Nanopore-derived variants were filtered to retain only variants supported by >95% of reads. Filtered VCF files were further processed using bcftools and custom Python scripts to standardize variant representation and extract genomic position, reference and alternate alleles, variant type, and allele frequency. Final variant datasets derived from Sanger and Oxford Nanopore sequencing were integrated using a unified framework for comparative and downstream analyses.

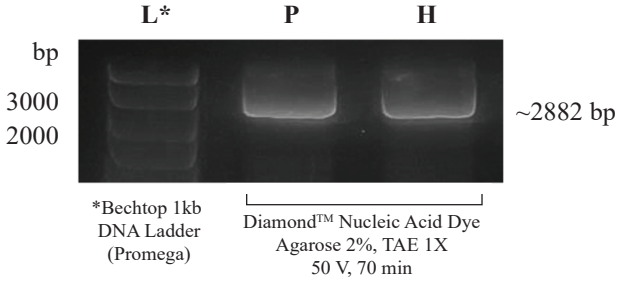

Figure 1. Agarose gel electrophoresis of HLA-B27 PCR amplicons before sequencing. A single band of approximately 2,882 bp was detected in the uveitis anterior patient sample (P) and healthy reference control (H), corresponding to the expected HLA-B27 amplicon size. L = BenchTop 1 kb DNA Ladder (Promega). Electrophoresis was performed on a 2% agarose gel in 1× TAE buffer stained with Diamond™ Nucleic Acid Dye and run at 50 V for 70 min.

Variant Mapping and Impact Analysis

Integrated variant datasets derived from Sanger and Oxford Nanopore sequencing were analyzed using a custom bioinformatics pipeline. Analyses included 13 anterior uveitis samples and 2 healthy reference samples, with cohort-level variant frequency calculations based on the 13 subjects samples. The frequency of each variant was quantified using variant prevalence (VP), defined as the proportion of sequencing sample harbouring the mutant allele relative to the total sample at the corresponding genomic position, with the formula as follows: [VP = Number of Samples Harboring the Variant / Total Number of Samples in the Cohort]. Reference control samples were retained for comparative analyses.

Variants were mapped to genomic coordinates relative to the *HLA-B27* reference sequence (GenBank accession number X03945.1) (22) and annotated according to genomic context, including promoter, exonic 1–7, intronic, and intergenic regions. Variants were further classified as single-nucleotide variants (SNVs) or insertion–deletion events, with SNVs categorized as transitions or transversions. Comparative profiling across patient and reference samples was used to distinguish recurrent, shared, sample-specific, and patient-enriched variants. To evaluate coding consequences, exon sequences were extracted according to reference coordinates and translated *in silico* using the reference reading frame. Variant effects were assessed using a codon-aware approach, in which multiple nucleotide changes occurring within the same codon were evaluated collectively to determine the net codon alteration and corresponding amino acid substitution. Polypeptide sequences derived from all samples were aligned to the reference sequence to identify conserved and altered residues, as well as shared and sample-specific amino acid changes.

To visualize and map the positions of missense variants across the HLA-B27 protein, a three-dimensional structural model was generated using AlphaFold3 (https://

alphafoldserver.com) and subsequently visualized and color-coded in PyMOL. Only regions with high prediction confidence (pLDDT>90) were included in the final structural representation to ensure reliable interpretation of variant localization.

Results

Demographic and Clinical Characteristics of Subjects

The demographic and clinical characteristics of the 13 subjects with anterior uveitis included in this study are summarized in Supplementary 1. Anterior uveitis subjects' age ranged from 26 to 63 years, with the majority being female (92.3%). Clinical examination revealed heterogeneous intraocular inflammatory manifestations, as reflected by inflammatory cell scores and flare scores in both the right eye (OD) and left eye (OS).

To further characterize the distribution of these clinical parameters across the cohort, descriptive statistical analyses were performed (Supplementary 2). For inflammatory cell scores, the mean value was slightly higher in OD (0.654) than in OS (0.577), while the median values were 0.000 and 0.500, respectively. Inflammatory cell scores ranged from 0.000 to 3.000 in OD and from 0.000 to 2.000 in OS. The OD group exhibited a higher standard deviation (SD=1.028) and coefficient of variation (CV=157.29%) than the OS group (SD=0.641; CV=111.02%). The interquartile range (IQR) was 1.000 for both eyes. The 95% confidence interval (CI) of the mean ranged from 0.095 to 1.213 in OD and from 0.229 to 0.925 in OS.

For flare scores, the mean value was higher in OS (0.692) than in OD (0.577). Median flare scores were 0.000 in OD and 1.000 in OS. Flare values ranged from 0.000 to 3.000 in OD and from 0.000 to 1.000 in OS. The OD group demonstrated greater variability (SD=0.954; CV=165.37%) than the OS group (SD=0.435; CV=62.81%). The IQR values were 1.000 and 0.500 for OD and OS, respectively. The 95% CI ranged from 0.058 to 1.096 for OD and from 0.456 to 0.929 for OS. Comparison of paired eyes using the Wilcoxon Signed-Rank Test revealed no statistically significant differences between OD and OS for inflammatory cell scores (p=0.831) or flare scores (p=0.546).

Distribution of Serum HLA-B27 Concentrations

To characterize the serological profile of HLA-B27 in the study cohort, serum HLA-B27 concentrations were quantified using ELISA and compared between subjects with anterior uveitis and healthy controls (Figure 2). Serum HLA-B27 concentrations were markedly higher in subjects with anterior uveitis compared to healthy controls. Overall, HLA-B27 levels in the anterior uveitis group spanned a broad range (0.90 to 7.40 ng/mL), with a median of 1.36 ng/mL. In contrast, concentrations in healthy controls remained consistently low, generally ranging from 0.39 to 0.44 ng/mL, with a median 0.42 ng/mL. These differences are visualized on a log10-transformed scale to accommodate the wide dynamic range of measurements across samples.

The distribution of HLA-B27 concentrations also differed notably between groups. Subjects with anterior uveitis exhibited a much wider spread of values, reflected by a larger interquartile range (IQR=3.48) and the presence of higher individual measurements. In contrast, the healthy control group showed a very compact distribution. This was further supported by the higher coefficient of variation observed in the anterior uveitis group (84.2%) compared to controls (7.1%), indicating significantly greater variability in HLA-B27 levels among anterior uveitis suubjects than in the stable, low-level measurements of the healthy control.

Statistical analysis confirmed a significant difference between groups (Welch's t-test, p=0.003). The anterior uveitis group exhibited substantially higher HLA-B27 concentrations, and the magnitude of this difference was

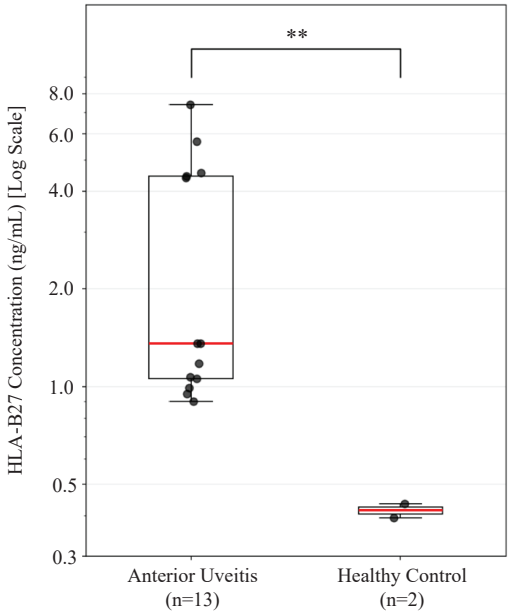

Figure 2. Comparison of HLA-B27 concentration between anterior uveitis subjects and healthy controls. Serum HLA-B27 levels are elevated in patients with anterior uveitis compared to controls. Data are presented as box-and-whisker plots showing the median (red line), interquartile range (box), and range (whiskers), with individual data points overlaid. A log10-transformed y-axis is used to accommodate the wide dynamic range of concentrations. A significant difference between groups was observed (**p<0.01).

substantial (Cohen's $d = 1.06$), reflecting a clear separation between groups. Consistent with this, the 95% confidence intervals (95% CI) did not overlap, with the anterior uveitis group ranging from 1.36 to 4.08 ng/mL and the control group from 0.15 to 0.68 ng/mL. These findings indicated that elevated HLA-B27 concentrations are consistently observed among anterior uveitis subjects compared to the stable, low-level distribution in healthy controls.

Distribution, Frequency, and Functional Impact of *HLA-B27* Variants

The distribution and characteristics of variants in the *HLA-B27* gene across the study cohort were summarized in Figure 3. Variants were identified throughout the promoter and coding region (exons 1–7). The spatial distribution was non-uniform, with a pronounced clustering in exon 2 and exon 3, where the highest density of variants was observed compared to other regions of the gene. Consistent with this pattern, variant frequency analysis revealed substantial heterogeneity across loci. While many variants occurred at low frequencies, several loci demonstrated moderate to high recurrence, with normalized frequencies higher than 0.70. These recurrent variants were predominantly located within exon 2, with additional occurrences in exon 3, indicating the presence of shared variant hotspots across the cohort. Additionally, several variants detected in anterior uveitis samples were also identified in healthy control samples.

Impact classification further showed that missense variants constituted the majority of detected variants, followed by smaller proportions of synonymous, intronic, frameshift, and promoter variants. Missense variants were primarily concentrated within exon 2 and exon 3, aligning with the regions of highest variant density and recurrence. Notably, several frameshift variants were identified within exon 2, indicating the presence of insertion–deletion events affecting the coding sequence. In addition to coding regions, variants were also identified in non-coding regions, especially the promoter region. A promoter-associated variant was observed within a specific position and was detected in 15.4% of the cohort, indicating a recurrent but lower-frequency variant. Variants were also detected within intronic regions; however, these were more broadly distributed and occurred at positions distal to canonical splice sites and other regulatory elements. As these variants are located deep within introns and are not expected to directly affect coding or proximal regulatory regions important for splicing, they are not displayed in the lollipop plot.

Overall, the lollipop plot highlights three key findings: i) a concentrated distribution of variants within exon 2 and exon 3, ii) the presence of several moderately to highly recurrent variants across the cohort, and iii) a dominant contribution of missense mutations relative to other variant types. These results provide a comprehensive overview of the genomic variation pattern of *HLA-B27* in the studied population.

Identification of *HLA-B27* Genetic Variants in Anterior Uveitis

Targeted sequencing of the *HLA-B27* gene identified multiple sequence variants across the study cohort. Variants that were also detected in healthy reference samples were considered shared background polymorphisms and were therefore excluded from focused downstream analysis. Comparative filtering initially identified 43 variants uniquely observed in anterior uveitis samples. To prioritize recurrent variants with broader representation within the cohort, downstream analyses focused primarily on variants shared by at least 30.8% of patient samples. Nevertheless, several low-frequency insertion-deletion events (indels) detected in less than 30.8% of the cohort were also retained because of their potential to cause alterations within the *HLA-B27* coding sequence. On this basis, a total of 13 prioritized variants were selected for further characterization (Table 4). The retained variants comprised seven SNVs, four insertions, and two deletions. These variants were distributed across the promoter region, exon 2, exon 3, and exon 4, with the majority localized within exon 2 and exon 3.

Among the identified SNVs, transitions were slightly more frequent than transversions. Several coding SNVs resulted in amino acid substitutions (missense variants), including D → S at codon 77, L → R at codon 82, V → L at codon 103, Y → H at codon 113, and I → V at codon 194. Two synonymous variants were also detected in exon 3 at positions 1256 and 1373. In addition to SNVs, multiple indels were identified within the coding region of exon 2, including single-nucleotide deletions at positions 849 and 918, as well as single-nucleotide insertions at positions 852 and 916. Because these indels involve the gain or loss of a single nucleotide within coding codons, they are generally predicted to alter the downstream translational reading frame. Notably, several samples exhibited adjacent insertion and deletion events in proximity, which may partially restore the original reading frame and thereby reduce the extent of downstream coding disruption. A promoter-region insertion at position 468 was additionally identified and classified as a potential transcription-related variant.

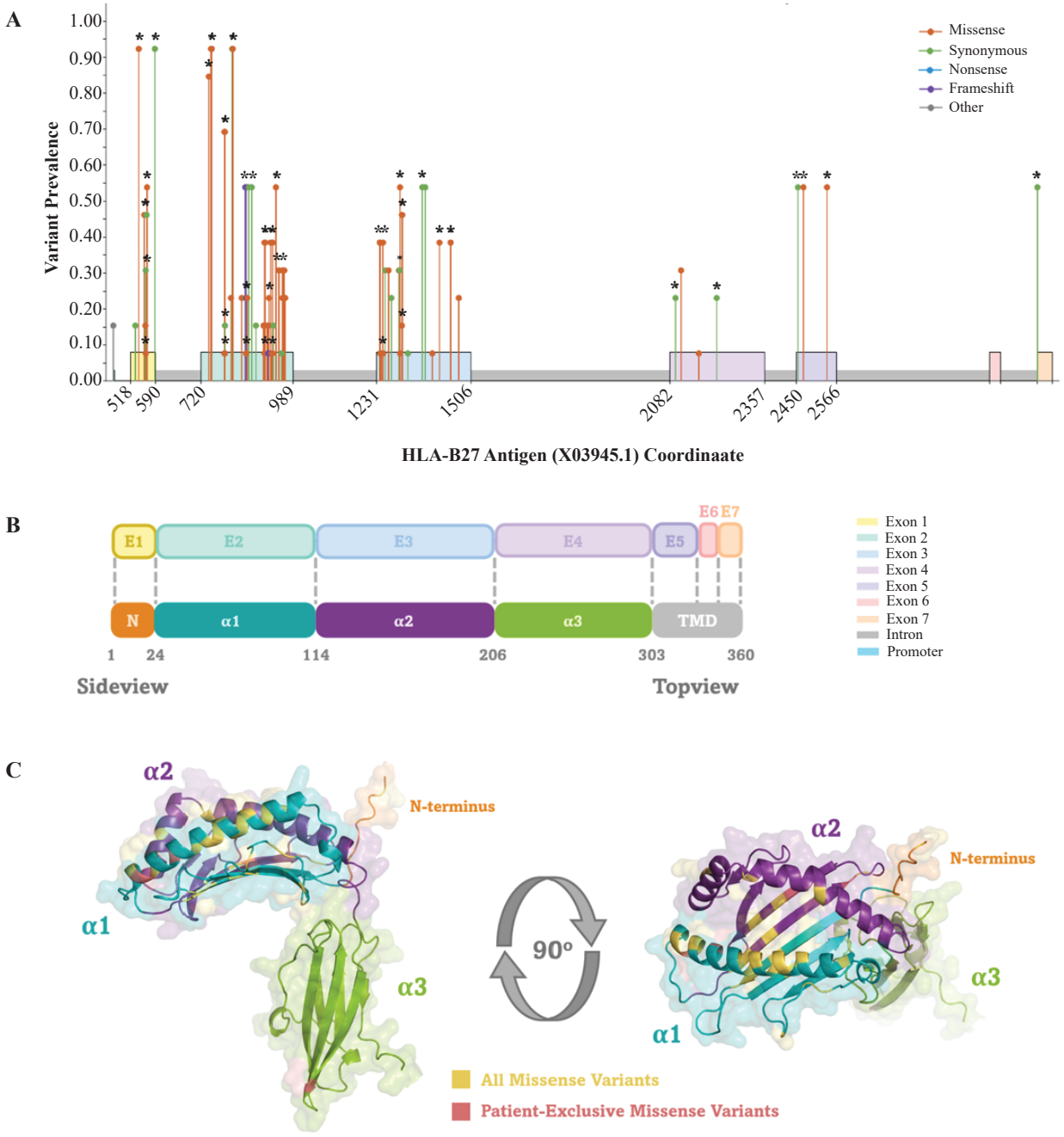

Figure 3. Distribution and structural localization of *HLA-B27* variants identified in patients with anterior uveitis. A: Lollipop plot showing the distribution, prevalence, and predicted functional impact of *HLA-B27* variants across the gene locus. Variant positions are mapped to the HLA-B27 reference sequence (GenBank accession X03945.1), with variant prevalence represented on the y-axis. Each lollipop corresponds to a detected variant, where the vertical stem indicates its genomic position and the dot height reflects its prevalence within the cohort. Variants are color-coded according to their functional class. Lollipops marked with an asterisk (*) indicate variants that were also detected in healthy control samples. The schematic along the x-axis illustrates the genomic organization of HLA-B27, including the promoter region, exons, and introns. Variants were detected throughout the gene but were more densely distributed within coding regions, particularly exons 2 and 3. B: The exon organization of the HLA-B27 gene (E1–E7) and the corresponding protein domains are shown. Exons 1–4 encode the N-terminal signal peptide (N), α1, α2, and α3 extracellular domains, whereas exons 5, 6, and 7 encode the transmembrane domain (TMD) and cytoplasmic tail. Amino acid positions of major protein domains are indicated below the schematic. (C) Structural model of HLA-B27, shown in side and top views (pLDDT>90). Protein domains are color-coded as follows: N-terminus (orange), α1 domain (teal), α2 domain (purple), and α3 domain (green). Residues corresponding to all identified missense variants are highlighted in yellow, whereas residues harboring missense variants detected exclusively in patients with anterior uveitis are highlighted in pink. In general, missense variants were found clustered within the peptide-binding pocket of HLA-B27, which is composed of domains α1 and α2, expressed by Exons 2 and 3, respectively. Due to the very low confidence (pLDDT 50) of the predicted model and the irregular conformation of the structure, the first 20 amino acids at the N-terminus, as well as the TMD and cytoplasmic tail, were omitted from the visualization to improve structural clarity and to highlight the main domain of the HLA-B27 protein.

Table 4. Characteristics of HLA-B27 gene mutations and variants identified in the study cohort.

Type	Position Ref	Location	Change	Codon Position	Impact	Total Samples	Variant Prevalence
Insertion	468	Promoter	C → CTTT	-	Transcription	2	0.154
Deletion	849	Exon 2	GA → G-	44	Frameshift	7	0.538
Insertion	852	Exon 2	A → AC	45	Frameshift	7	0.538
Insertion	852	Exon 2	A → AT	45	Frameshift	3	0.231
Insertion	916	Exon 2	C → CA	66	Frameshift	1	0.077
Deletion	918	Exon 2	GC → G-	67	Frameshift	1	0.077
Transition	948	Exon 2	A → G	77	Missense (D → S)	4	0.308
Transversion	963	Exon 2	T → G	82	Missense (L → R)	4	0.308
Transition	1256	Exon 3	T → C	99	Synonymous	4	0.308
Transversion	1266	Exon 3	G → C	103	Missense (V → L)	4	0.308
Transition	1296	Exon 3	T → C	113	Missense (Y → H)	4	0.308
Transversion	1373	Exon 3	G → C	138	Synonymous	7	0.538
Transition	2114	Exon 4	A → G	194	Missense (I → V)	4	0.308

Variant allele frequencies ranged from 0.077 to 0.538. The highest-frequency variants included the deletion at position 849, the insertion at position 852 (A→AC), and the synonymous transversion at position 1373, each detected with a VP of 0.538. Several recurrent missense variants, including D → S at position 948, L → R at position 963, V → L at position 1266, Y → H at position 1296, and I → V at position 2114, were each detected with a VP of 0.308. Lower-frequency frameshift-associated indels were observed at positions 916 and 918, each with a VP of 0.077.

Discussion

Several important findings emerged from the present study. Subjects with anterior uveitis exhibited significantly elevated serum HLA-B27 antigen levels compared with healthy reference controls based on Sandwich ELISA analysis. Complementing these serological findings, targeted sequencing initially identified 43 anterior uveitis subjects-exclusive variants across the *HLA-B27* locus after exclusion of shared polymorphisms detected in healthy references. Subsequent analyses focused on 13 selected variants with potential relevance within the cohort, consisting predominantly of missense SNVs, several coding-region indels that may affect the translational reading frame, and a promoter-region insertion potentially associated with transcriptional regulation. These variants were concentrated primarily within exons 2 and 3 rather than being uniformly distributed across the gene. Collectively, these findings may suggest that both quantitative and sequence-level variation in *HLA-B27* contribute to the molecular landscape of anterior uveitis within this cohort.

The clinical findings revealed substantial heterogeneity in intraocular inflammatory manifestations among subjects with anterior uveitis, as reflected by the broad distribution of inflammatory cell and flare scores and the high coefficients of variation observed across the cohort. This variability is consistent with the heterogeneous clinical spectrum of HLA-B27-associated anterior uveitis, in which disease severity may differ among individuals due to variations in disease stage, inflammatory duration, treatment history, and host immune responses.(11-14) Despite this heterogeneity, the overall inflammatory burden remained predominantly mild to moderate, as indicated by the low median inflammatory cell and flare scores and the relatively narrow 95% confidence intervals. No statistically significant differences were observed between the right and left eyes for either parameter, suggesting a comparable distribution of inflammatory activity between paired eyes. Collectively, these findings may suggest that the cohort encompasses clinically relevant yet heterogeneous inflammatory phenotypes, thereby supporting further investigation of potential associations between ocular inflammation, serum HLA-B27 antigen levels, and *HLA-B27* genetic variation.

The significantly elevated serum HLA-B27 antigen levels (Figure 2) observed in subjects with anterior uveitis may suggest an association between active disease and altered circulating HLA-B27 abundance. Although the present study did not investigate the transcriptional regulation, cellular expression, or tissue localization of HLA-B27, inflammatory conditions are known to enhance MHC class I expression through cytokine-mediated

pathways, particularly interferon-γ signaling, and may increase circulating soluble HLA molecules through cellular turnover or membrane shedding.(1,14,16) Within the context of anterior uveitis, elevated serum HLA-B27 may therefore reflect an immunologically activated state that could contribute to antigen presentation and the maintenance of inflammatory responses.(1,20,21) Accordingly, the present findings may suggest that HLA-B27 functions not only as a susceptibility marker but may also participate in the inflammatory processes associated with anterior uveitis.

The non-random distribution of variants (Figure 3), with a clear predominance in exon 2 and exon 3, is biologically notable because these regions encode the α1 and α2 domains that form the peptide-binding groove of the HLA-B27 molecule.(13,16) In HLA class I genes, sequence diversity is often enriched within peptide-binding domains, where amino acid variation can alter peptide affinity, repertoire selection, and subsequent recognition by $CD8^+$ T cells or other immune receptors.(13,14) The concentration of variants within these exons may therefore suggest that the detected changes are located in structurally and immunologically relevant regions rather than being randomly distributed across the gene. In the context of anterior uveitis, such variation may influence the presentation of self- or microbial-derived peptides, potentially contributing to aberrant immune activation in genetically susceptible individuals.(3,20) Collectively, these findings are consistent with the concept that variation within peptide-binding domains may represent an important component of HLA-B27-associated inflammatory disease biology.(14,16,17)

Initial variant calling was performed by aligning anterior uveitis subjects-derived and healthy reference *HLA-B27* sequences to the GenBank reference sequence X03945.1 (22), revealing a broad spectrum of variation across the *HLA-B27* locus, including both anterior uveitis subjects-exclusive variants and variants shared with healthy reference samples (Figure 3). Many detected variants were present in both groups and were therefore interpreted as shared polymorphisms rather than changes uniquely associated with anterior uveitis. Because healthy reference participants showed no clinical manifestations of anterior uveitis and exhibited lower serum HLA-B27 antigen levels than affected anterior uveitis subjects, these shared variants may be less likely to represent disease-specific alterations within the context of the present dataset.(20,21) This observation is consistent with the extensive allelic diversity of HLA class I genes, including *HLA-B27*, which are among the most polymorphic loci in the human genome.(10,13-15,17) However, publicly available data describing HLA-B27 diversity in Indonesian populations remain limited, restricting definitive classification of some shared variants as population-specific polymorphisms.(10,15) Given the potential contribution of population-related sequence diversity, distinguishing shared polymorphisms from anterior uveitis subjects-restricted variants was an important analytical step. Accordingly, downstream analyses focused on the 13 variants identified exclusively in subjects with anterior uveitis, as these variants may be more relevant to the disease context within this cohort.

Among the 13 anterior uveitis subjects-exclusive variants prioritized in this study, 7 were SNVs, including five missense and two synonymous variants. The predominance of missense changes is biologically notable because these variants alter the amino acid sequence of *HLA-B27* and may therefore have greater potential to affect protein function than synonymous substitutions.(14,16,17) Several recurrent missense variants were detected in approximately 30.8% of patient samples, including D → S at codon 77, L → R at codon 82, V → L at codon 103, Y → H at codon 113, and I → V at codon 194. These substitutions cluster within the α1 domain of *HLA-B27*, a region involved in the peptide-binding groove and immune receptor interface, suggesting that amino acid changes at these positions may influence peptide-binding specificity and affinity.(14,15,23) The identified variants encompass both non-conservative and conservative amino acid substitutions with potentially distinct physicochemical consequences. D → S at codon 77 and Y → H at codon 113 involve changes in electrostatic and hydrogen-bonding properties, which may alter local molecular interactions and surface chemistry.(24-26) In contrast, L → R at codon 82 introduces a larger positively charged residue in place of a hydrophobic residue and may therefore affect local packing architecture or receptor-facing molecular surfaces, whereas V → L at codon 103 and I → V at codon 194 represent more conservative hydrophobic substitutions that may exert comparatively subtler effects on steric arrangement, conformational flexibility, or protein conformation.(23-25) Collectively, these findings may suggest that the identified substitutions have varying degrees of potential structural impact on HLA-B27, with non-conservative changes potentially exerting greater effects on peptide repertoire selection, molecular stability, receptor recognition, or intracellular folding than conservative substitutions, thereby potentially contributing to inflammatory susceptibility in anterior uveitis.(14,16,17,24-27)

In addition to SNVs, several patient-exclusive indels were identified within both coding and regulatory

regions of the HLA-B27 locus, including single-nucleotide deletions at codons 44 (53.8%) and 67 (7.7%), single-nucleotide insertions at codons 45 (A → AC, 53.8%; A → AT, 23.1%) and 66 (7.7%), and a promoter-region insertion upstream of the coding sequence (15.4%). Because the biological consequences of indels depend on both their genomic location and length, variants occurring in coding and regulatory regions may affect gene biology through distinct mechanisms.(28,29) Within coding regions, single-nucleotide indels may shift the translational reading frame and generate aberrant protein sequences or premature termination codons, whereas indels involving multiples of three nucleotides generally preserve the reading frame.(30,31) As all coding-region indels identified in this cohort involved gain or loss of a single nucleotide, they may possess the potential for frameshift-related disruption. However, several samples exhibited adjacent insertion–deletion pairs that may have restored the downstream reading frame despite local sequence alterations.(27-31)

Detailed analysis showed that coding-region indels were not uniformly distributed across the cohort and frequently occurred as adjacent insertion–deletion pairs. The most common pattern, detected in 38.5% of samples, involved concurrent deletion at codon 44 and insertion at codon 45 (A → AC), while 7.7% carried the same deletion together with the A → AT insertion. An additional 7.7% of samples exhibited concurrent insertion and deletion events at codons 66 and 67, respectively. Because these paired indels may compensate for one another at the reading-frame level, they could limit extensive downstream sequence disruption despite local amino acid alterations near the affected codons.(27,29-31) In contrast, isolated indels were also observed, including a deletion at codon 44 (7.7%) and insertions at codon 45 involving A → AC and A → AT (15.4% each). As these variants lacked nearby compensatory indels, they may be more likely to produce true downstream frameshift alterations and substantial changes to the encoded amino acid sequence. Overall, adjacent compensatory indels and independently occurring single-nucleotide indels were detected in approximately 38.5% and 30.8% of the cohort, respectively, suggesting that both reading-frame restoration and frameshift-prone configurations represent recurrent features of the coding-region indels identified.(27-32)

Frameshift events within exon 2 may reduce production of a stable full-length HLA-B27 heavy chain, disrupt formation of the α1 domain within the peptide-binding groove, impair association with β2-microglobulin, or decrease cell-surface expression.(14,16,17,23) Misfolded or truncated products may also be retained and degraded through intracellular quality-control pathways rather than reaching the plasma membrane. Although such effects could reduce conventional antigen presentation, intracellular accumulation or aberrant processing of unstable HLA-B27 species may potentially influence endoplasmic reticulum stress and inflammatory signaling pathways implicated in other HLA-B27-associated disorders.(16,17,27,32) In contrast, the promoter-region insertion would not be expected to alter the coding sequence directly but may affect transcription factor binding, promoter activity, or chromatin accessibility, potentially modulating HLA-B27 expression levels rather than protein structure.(28,29,33)

Several limitations should be considered when interpreting the present findings. First, the cohort was relatively small and derived from a single-center Indonesian population, which may limit generalizability and the ability to capture rare or population-specific *HLA-B27* variants. Second, the number of healthy reference samples was limited, and inclusion of larger ethnically matched control datasets may improve discrimination between background polymorphisms and variants potentially enriched in anterior uveitis. Third, the study was based primarily on serological and sequence-level analyses without direct assessment of transcript abundance, allele-specific expression, protein folding, cell-surface localization, peptide-binding properties, or downstream immune responses. Consequently, the biological significance of the identified variants remains largely predictive, and direct functional effects on HLA-B27 biology or disease pathogenesis cannot yet be established. Although several substitutions and coding-region indels may influence molecular stability, peptide presentation, or intracellular protein handling, these effects were not experimentally validated. Future studies incorporating larger multi-center cohorts, expanded population controls, high-resolution HLA haplotyping, transcriptomic and proteomic analyses, structural modeling, peptide-binding studies, promoter assays, and functional immunological investigations may help determine whether the identified variants contribute to HLA-B27 biology and the clinical heterogeneity of anterior uveitis.

Conclusion

The identification of elevated circulating HLA-B27 antigen levels and recurrent variants within functionally important regions of the *HLA-B27* gene highlights substantial molecular heterogeneity among anterior uveitis patients. Patients exhibited higher serum HLA-B27 antigen levels

than healthy reference controls, and sequencing identified 13 recurrent patient-exclusive variants, predominantly located within exons 2 and 3 of the *HLA-B27* gene, including both single-nucleotide substitutions and insertion–deletion events. Notably, these variants were concentrated within regions encoding key structural and immunological domains of HLA-B27, highlighting substantial molecular heterogeneity within this anterior uveitis cohort. Overall, these findings establish a foundation for future studies involving larger multicenter cohorts and integrated transcriptomic, structural, and immunological analyses to elucidate further the molecular and clinical implications of *HLA-B27* variation in anterior uveitis.

Acknowledgments

The authors gratefully acknowledge the laboratory staff of Cicendo National Eye Hospital and the School of Life Sciences and Technology, Institut Teknologi Bandung, for their technical support in blood collection, sample processing, and laboratory procedures. This study was supported by a research grant from Cicendo National Eye Hospital, Bandung. Additional support in the form of research consumables and laboratory infrastructure was provided by the School of Life Sciences and Technology, Institut Teknologi Bandung.

Authors Contribution

SA contributed to study conceptualization, methodology development, patient/sample recruitment coordination, data acquisition and collection, laboratory investigation, data curation, formal analysis, visualization, figure preparation, and original manuscript drafting. AAM is an ophthalmologist at the Outpatient Department of Infection and Immunology and a uveitis specialist who examined the eyes and recruited anterior uveitis patients for this study. AF, PM, EAI is an ophthalmologist at the Outpatient Department of Infection and Immunology who examined the eyes and recruited anterior uveitis patients for this study. EG contributed to study conceptualization, clinical supervision, patient evaluation, and sample collection oversight, methodology input, data interpretation, formal analysis, manuscript review, and overall project supervision. ER contributed to study conceptualization, methodology development, data analysis strategy, interpretation of findings, manuscript review and editing, and academic supervision of the project. MIT contributed to study conceptualization, methodology development, data analysis strategy, interpretation of findings, manuscript review and editing, resource support, and academic supervision of the project. MH contributed to data processing, bioinformatic and statistical analysis, data interpretation, visualization, figure design, and manuscript writing and editing. All authors critically reviewed the manuscript, approved the final version, and agreed to be accountable for all aspects of the work.

Ethical Statement

This study was conducted in accordance with the principles of the Declaration of Helsinki. The study protocol was reviewed and approved by the Health Research Ethics Committee of Cicendo National Eye Hospital, Bandung, Indonesia (Approval No. LB.02.01/2.3/761/2023).

Conflict of Interest

The authors declare no conflicts of interest or competing interests related to the content of this manuscript.

References

1. Egwuagu CE, Alhakeem SA, Mbanefo EC. Uveitis: Molecular pathogenesis and emerging therapies. Front Immunol. 2021; 12: 623725. doi: 10.3389/fimmu.2021.623725.
2. Jabs DA, Nussenblatt RB, Rosenbaum JT; Standardization of Uveitis Nomenclature (SUN) Working Group. Standardization of uveitis nomenclature for reporting clinical data: Results of the First International Workshop. Am J Ophthalmol. 2005; 140(3): 509–16.
3. Martin TM, Rosenbaum JT. An update on the genetics of HLA-B27-associated acute anterior uveitis. Ocul Immunol Inflamm. 2011; 19(2): 108–14.
4. Hou S, Li N. Uveitis genetics. Exp Eye Res. 2020; 190: 107853. doi: 10.1016/j.exer.2019.107853.
5. Antoniou AN, Lenart I, Guiliano DB, Powis SJ. Pathogenicity of misfolded and dimeric HLA-B27 molecules. Int J Rheumatol. 2011; 2011: 486856. doi: 10.1155/2011/486856.
6. Shaw J, Hatano H, Kollnberger S. The biochemistry and immunology of non-canonical forms of HLA-B27. Mol Immunol. 2014; 57(1): 52–8.
7. Thorne JE, Suhler E, Skup M, Tari S, Macaulay D, Chao J, *et al.* Prevalence of noninfectious uveitis in the United States: A claims-based analysis. JAMA Ophthalmol. 2016; 134(11): 1237–45.
8. Gelfman S, Moscati A, Huergo SM, Wang R, Rajagopal V, *et al.* A large meta-analysis identifies genes associated with anterior uveitis. Nat Commun. 2023; 14: 43036. doi: 10.1038/s41467-023-43036-1.
9. Dick AD, Tundia N, Sorg R, Zhao C, Chao J, Joshi A, *et al.* Risk of ocular complications in patients with noninfectious intermediate uveitis, posterior uveitis, or panuveitis. Ophthalmology. 2016;

123(3): 655–62.
10. Robinson J, Barker DJ, Georgiou X, Cooper MA, Flicek P, Marsh SGE. IPD-IMGT/HLA Database. Nucleic Acids Res. 2020; 48(D1): D948–D955.
11. Ayu K, Sari D, Ketut N, Susila N, Budhiastra P. Karakteristik pasien uveitis di Rumah Sakit Umum Pusat Sanglah Denpasar periode Maret 2016 sampai Desember 2016. J Medika Udayana. 2019; 8(8): 1–9.
12. Hosomichi K, Shiina T, Tajima A, Inoue I. The impact of next-generation sequencing technologies on HLA research. J Hum Genet. 2015; 60(11): 665–73.
13. Klasberg S, Surendranath V, Lange V, Schofl G. Bioinformatics strategies, challenges, and opportunities for next-generation sequencing-based HLA genotyping. Transfus Med Hemother. 2019; 46(5): 312–24.
14. Bowness P. HLA-B27. Annu Rev Immunol. 2022; 40: 167–95.
15. Luo Y, Kanai M, Choi W, Li X, Sakaue S, Yamamoto K, *et al.* A high-resolution HLA reference panel capturing global population diversity. Nat Genet. 2021; 53(10): 1508–17.
16. Chen B, Li J, He C, Li D, Tong W, Zou Y. Role of HLA-B27 in disease pathogenesis. Mol Med Rep. 2023; 27(2): 1–10. doi :10.3892/mmr.2022.12867.
17. Colbert RA, Navid F, Gill T. The role of HLA-B27 in spondyloarthritis. Best Pract Res Clin Rheumatol. 2021; 35(3): 101661. doi: 10.1016/j.berh.2021.101661.
18. Chen S, Huang W, Wan Q, Tang Z, Li X, Zeng F, et al. Genome-wide and single-cell transcriptomic analysis in HLA-B27-associated uveitis. J Transl Med. 2024; 22(1): 271. doi: 10.1186/s12967-024-05000-0.
19. Ranganathan V, Gracey E, Brown MA, Inman RD, Haroon N. Pathogenesis of ankylosing spondylitis - Recent advances and future directions. Nat Rev Rheumatol. 2017; 13(6): 359–67.
20. Wakefield D, Clarke D, McCluskey P. HLA-B27 anterior uveitis: Recent advances. Front Immunol. 2021; 11: 608134. doi: 10.3389/fimmu.2020.608134.
21. Werkl P, Rademacher J, Pleyer U. HLA-B27-positive anterior uveitis: Clinical aspects and management. Ophthalmologie. 2024; 121(Suppl 1): 12–22.
22. Weiss EH, Kuon W, Dörner C, Lang M, Riethmüller G. Organization, sequence and expression of the HLA-B27 gene: A molecular approach to analyze HLA and disease associations. Immunobiology. 1985; 170(5): 367–80.
23. Madden DR. The three-dimensional structure of peptide-MHC complexes. Annu Rev Immunol. 1995; 13: 587–622.
24. Betts MJ, Russell RB. Amino acid properties and consequences of substitutions. In: Barnes MR, Gray IC, editors. Bioinformatics for Geneticists. Hoboken: Wiley; 2003. p. 289–316.
25. Branden C, Tooze J. Introduction to Protein Structure. 2nd ed. New York City: Garland Science; 1999.
26. Pace CN, Scholtz JM. A helix propensity scale based on experimental studies of peptides and proteins. Biophys J. 1998; 75: 422–27.
27. Kollnberger S, Bird L, Sun MY, Retiere C, Braud VM, McMichael A, *et al.* Cell-surface expression and immune receptor recognition of HLA-B27 homodimers. Arthritis Rheum. 2002; 46(11): 2972–82.
28. Corradin O, Scacheri PC. Enhancer variants: Evaluating functions in common disease. Genome Med. 2014; 6: 85. doi: 10.1186/s13073-014-0085-3.
39. Maston GA, Evans SK, Green MR. Transcriptional regulatory elements in the human genome. Annu Rev Genomics Hum Genet. 2006; 7: 29–59.
30. Seligmann H. Frameshift mutations and the genetic code. J Mol Evol. 2012; 75: 201–10.
31. Pagani F, Baralle FE. Genomic variants in exons and introns: identifying the splicing spoilers. Nat Rev Genet. 2004; 5(5): 389–96.
33. Ellgaard L, Helenius A. Quality control in the endoplasmic reticulum. Nat Rev Mol Cell Biol. 2003; 4(3): 181–91.
33. Vockley CM, D'Ippolito AM, McDowell IC, Majoros WH, Safi A, Song L, *et al*. Direct GR binding sites potentiate clusters of TF binding across the human genome. Cell. 2016; 166(5): 1269–81.